Electronic Supplementary Information

Two Nickel-Added Poly(polyoxometalate)s Built by Keggin-Type {Ni$_6$PW$_9$} and Anderson-Type NiW$_6$O$_{24}$ *via* WO$_4$/Sb$_2$O Bridges and Ni–O–W Linkages with Efficient Hydrogen Evolution Activity

Peng-Yun Zhang, Chen Lian, Zhen-Wen Wang, Juan Chen, Hongjin Lv* and Guo-Yu Yang*

MOE Key Laboratory of Cluster Science, School of Chemistry and Chemical Engineering, Beijing Institute of Technology, Beijing 102488.

*Corresponding Author(s): Guo-Yu Yang: ygy@bit.edu.cn; Hongjin Lv: hlv@bit.edu.cn

Table of Contents

Experimental Procedures

Materials and Instruments. The precursor $Na_9[A-\alpha-PW_9O_{34}]\cdot7H_2O$ and the photosensitizer $[Ir(coumarin)_2-(dtbbpy)]^+$ were prepared as literature reported.[1,2] All other chemicals with analytical grade utilized in this work were commercially obtained. SHG measurements were performed on a Q-switched Nd:YAG laser (1064 nm). Powder X-ray diffraction (PXRD) patterns were obtained by employing a Bruker D8 Advance diffractometer (Cu Kα radiation, λ=1.54056 Å). IR spectra were tested by a Nicolet iS10 FT-IR spectrometer with the wavenumber varying from 4000 to 400 cm^{-1}. The X-ray photoelectron spectroscopy (XPS) was measured by a PHI VersaProbe III device. Elemental analyses for C, H, and N were performed by a Perkin-Elmer 2400-II CHNS/O analyzer. ICP analyses of Ni, Sb, and W were conducted on a Perkin–Elmer Optima 2000 ICP-AES spectrometer. UV–Vis diffuse- reflectance spectra were collected on a Perkin-Elmer Lambda 750 S spectrometer. TG analyses were recorded on a Mettler Toledo instrument from 25 to 700 °C.

X-ray Crystallography. The size-suitable and high-quality single crystals of **1** and **2** were picked out and stuck to the top of glass thread for collecting diffraction data on the Bruker APEX II CCD detector (Mo Kα radiation, λ=0.71073 Å) at room temperature. In the OLEX2 interface, the structures of **1** and **2** were determined by using the intrinsic phasing method through the ShelXT program and further refined by employing full-matrix least-squares on F^2 through the SHELXL program.[3–5] In the process of refinement, all non-hydrogen atoms of **1** and **2** were refined anisotropically, respectively. The hydrogen atoms attached to carbon and nitrogen atoms were geometrically placed and refined isotropically by using a riding model. The effect of disordered solvent molecules on the overall intensity data of the structures was processed by the Solvent Mask in the OLEX2 interface.[6] The "OMIT" commands were used to omit both weak diffraction data above 50 degrees and low-quality diffraction data with significant deviations for **1** and **2**. For compound **1**, the largest residual electron density peak is 5.27 e·Å^{-3}, with the Q-peak located extremely close to the N4 atom at an unreasonable position, leading to its non-attribution. According to the Fourier maps, 22 and 5 lattice water molecules (electron density peak > 5 e·Å^{-3}) have been found for compounds **1** and **2**, respectively. There were numerous short connections between O(water)…O, indicating extensive H-bonding interactions between them, alongside the high disorder of lattice water molecules within the channels of framework. In addition, there were some residual electron density peaks below 5 e·Å^{-3} remaining unassigned, leading to ambiguities in the precise location and quantity of lattice water molecules. Importantly, however, the absence of definitive attribution for these residual peaks does not compromise the accuracy of the final model for **1** and **2**. Based on the potential electron counts and solvent-accessible voids from the Solvent Mask reports, 17 and 40 lattice water molecules should be additionally added for **1** and **2**, respectively, and further verified by elemental analyses and TGA. The Flack factor of 0.33 for compound **2** is attributed to the presence of two different configurations in the structure, resulting in partial internal racemization.

Photocatalytic Hydrogen Evolution Experiments. The experiments were carried out in a mixed DMF/CH$_3$CN (6 ml, v/v, 3/1) solution containing **1** or **2** as catalysts, 0.3 mM $[Ir(coumarin)_2(dtbbpy)]^+$ as photosensitizer, 0.2 M triethanolamine (TEOA) as sacrificial electron donor, 2.5 M H$_2$O as proton source. The solution was degassed with Ar/CH$_4$ (v/v, 4/1) and the quartz photocatalytic reactor was placed in the multichannel photochemical reaction system of the Beijing Perfectlight PCX-50C instrument. Then illuminated by a white-light source (10 W, λ = 400–800 nm), and the reaction temperature was adjusted at 25 °C by a low-temperature thermostat bath. The

gas samples were analyzed by GC979011 gas chromatograph equipped with TCD and 5 Å molecular sieve column (3 m × 3 mm) with argon gas as carrier gas and quantified based on the internal CH_4 standard.
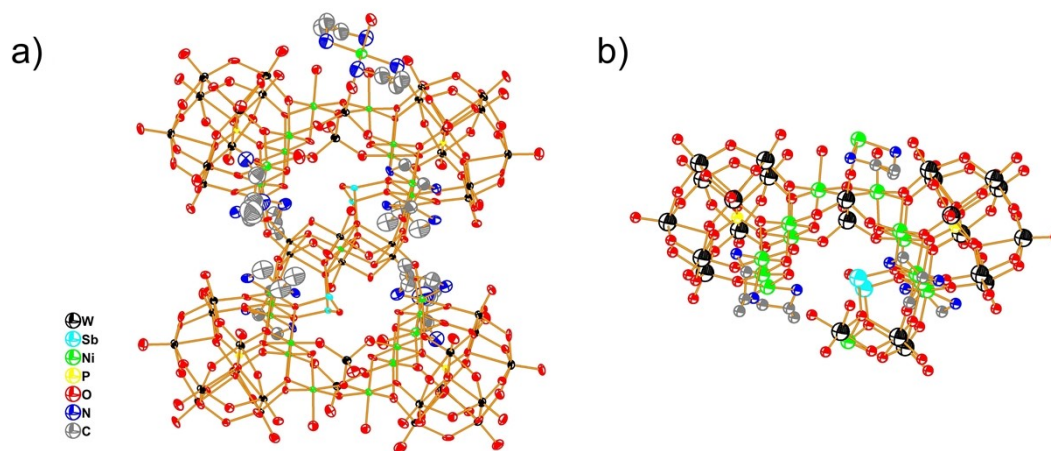
Fig. S1. (a) The structural unit and (b) asymmetrical unit of **1**.
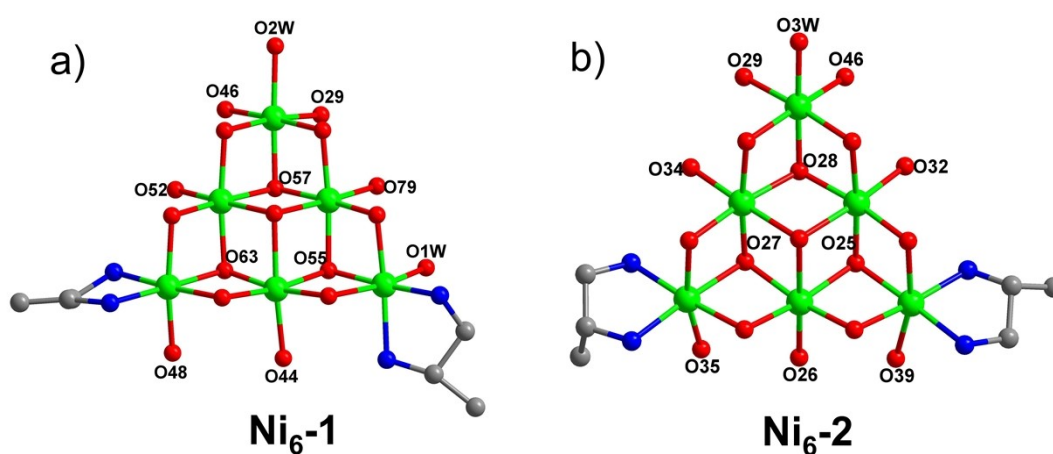
Fig. S2 (a) The **Ni₆-1** cluster of **1**. (b) The **Ni₆-2** cluster of **1**.
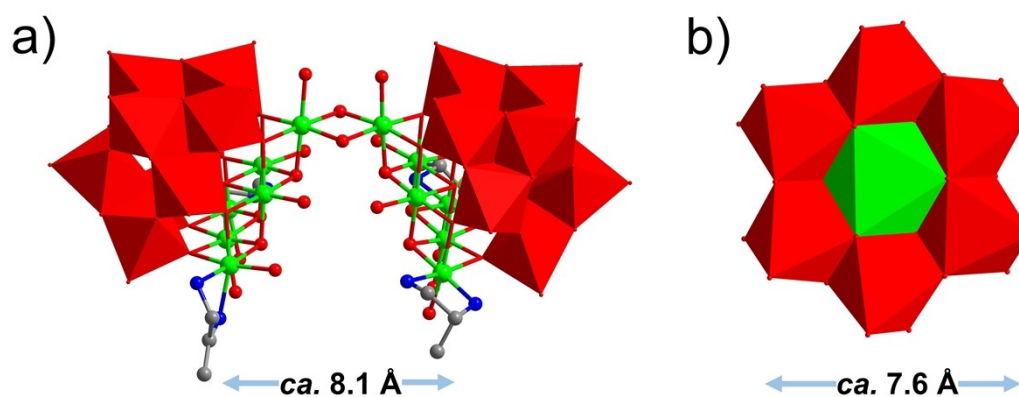
Fig. S3 (a) The distance between **Ni₆-1** and **Ni₆-2** units of **1**. (b) The diameter of the Anderson-type cluster of **1**.
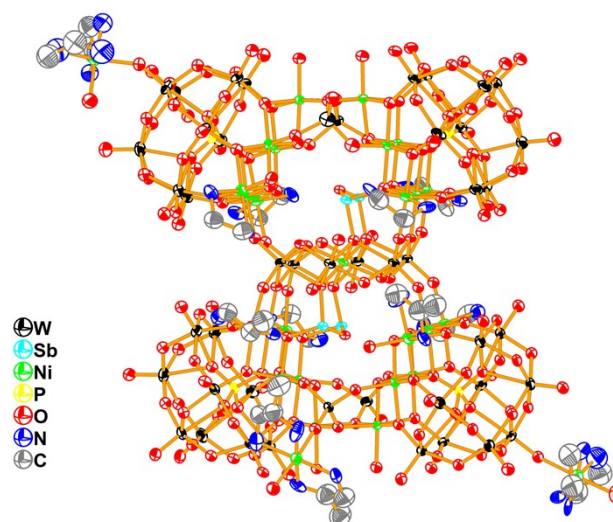
Fig. S4. The structural unit of **2**.
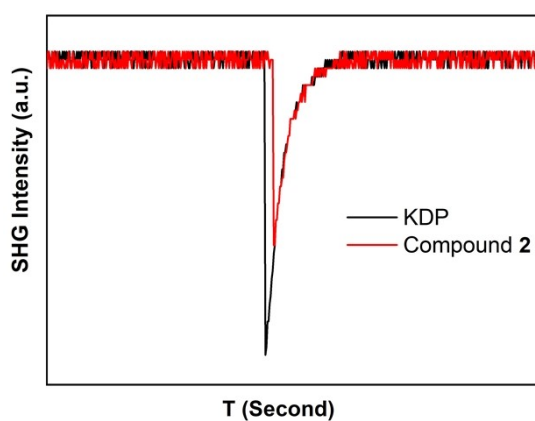
Fig. S5 The SHG oscilloscope traces signals of KDP and compound **2** in the same powder particle size (75–106 μm).
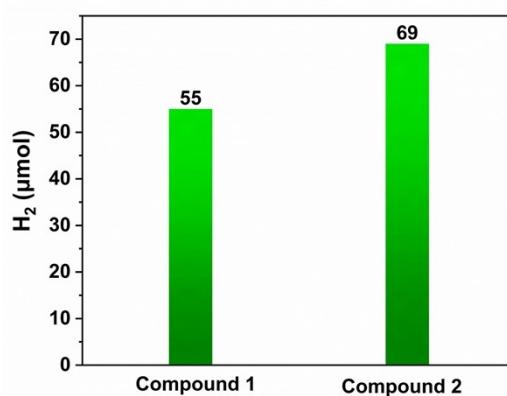
Fig. S6. The comparison of 1 mg of compounds **1** and **2** used for H_2 evolution. Conditions: white light (10 W, 400–800 nm), 0.3 mM [Ir(coumarin)$_2$(dtbbpy)]$^+$, 0.2 M TEOA, 2.5 M H_2O, 6 mL DMF/CH_3CN (v/v, 3:1) degassed with Ar/CH_4 (v/v, 4:1).
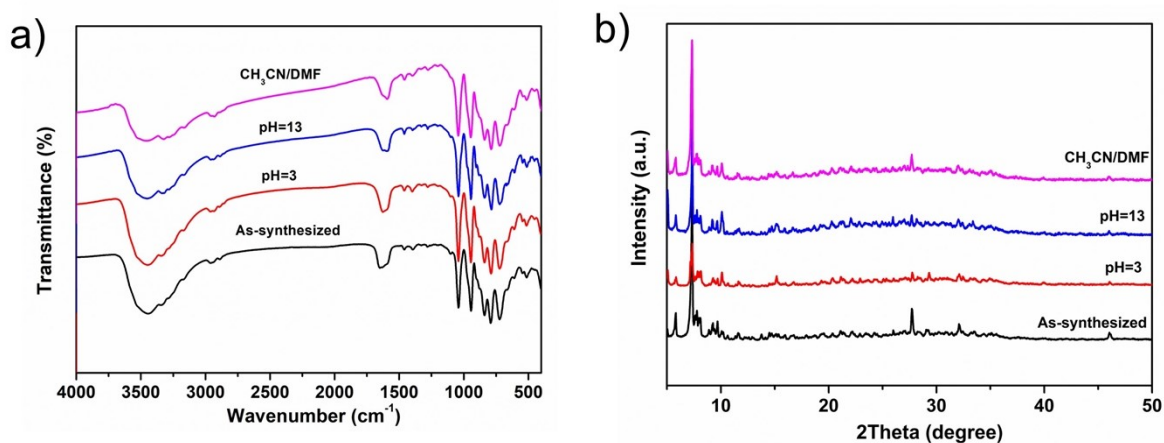
Fig. S7. The (a) IR Spectra and (b) PXRD patterns of catalyst **2** including freshly synthesized samples and samples immersed into different acidic/alkaline solutions and organic solvents for 24 h.
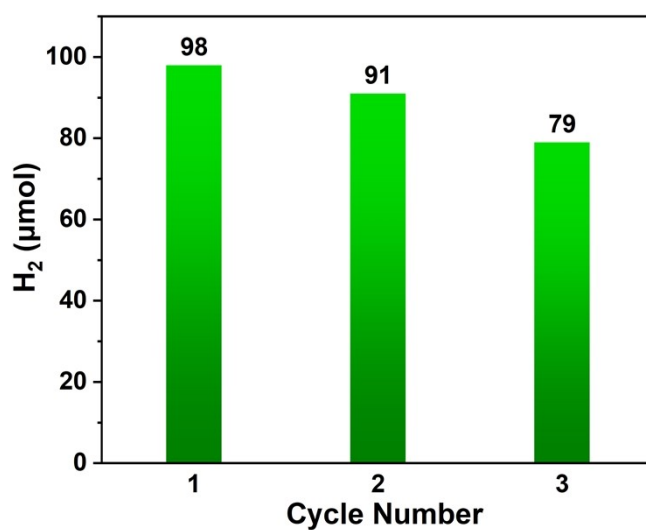
Fig. S8. The cyclic experiments for H_2 evolution with 2 mg of catalyst **2**. Conditions: white light (10 W, 400–800 nm), 0.3 mM [Ir(coumarin)$_2$(dtbbpy)]$^+$, 0.2 M TEOA, 2.5 M H_2O, 6 mL DMF/CH$_3$CN (v/v, 3:1) degassed with Ar/CH$_4$ (v/v, 4:1), reaction time: 5 h.
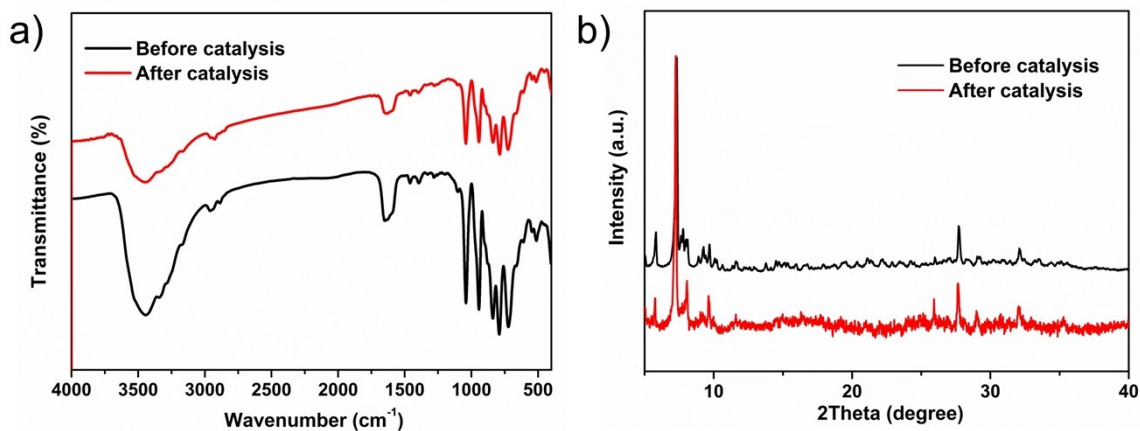
Fig. S9. The (a) IR Spectra and (b) PXRD patterns of **2** before and after catalysis.
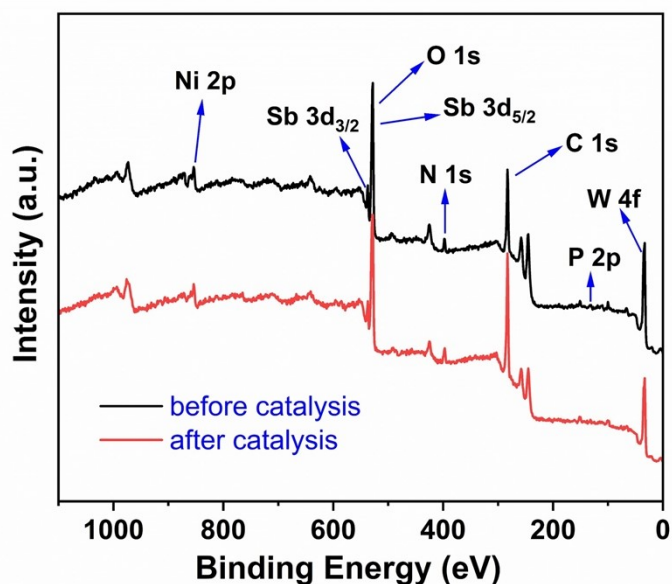
Fig. S10. The XPS full survey spectra of compound **2** before and after catalysis.

IR spectra. As shown in Fig. S11, characteristic absorption peaks can be observed at 1046, 949, 845–793, 722 cm^{-1} for compound **1** and 1040, 943, 835–792, 725 cm^{-1} for compound **2**, which are attributed to $v(P–O)$, $v(W–O_t)$, $v(W–O_b)$ and $v(W–O_c)$ respectively, indicating the existence of $[B\text{-}\alpha\text{-}PW_9O_{34}]^{9-}$ fragments. The stretching and bending vibration peaks attributed to –OH can be seen at 3446 cm^{-1}, 1622 cm^{-1} for compound **1** and 3450 cm^{-1}, 1636 cm^{-1} for compound **2**, respectively. In addition, the characteristic peaks observed at 2925 cm^{-1}, 1464–1403 cm^{-1} for compound **1,** and 2950 cm^{-1}, 1458–1391 cm^{-1} for compound **2** are attributed to $-NH_2$ and $-CH_2$ of organic amine.
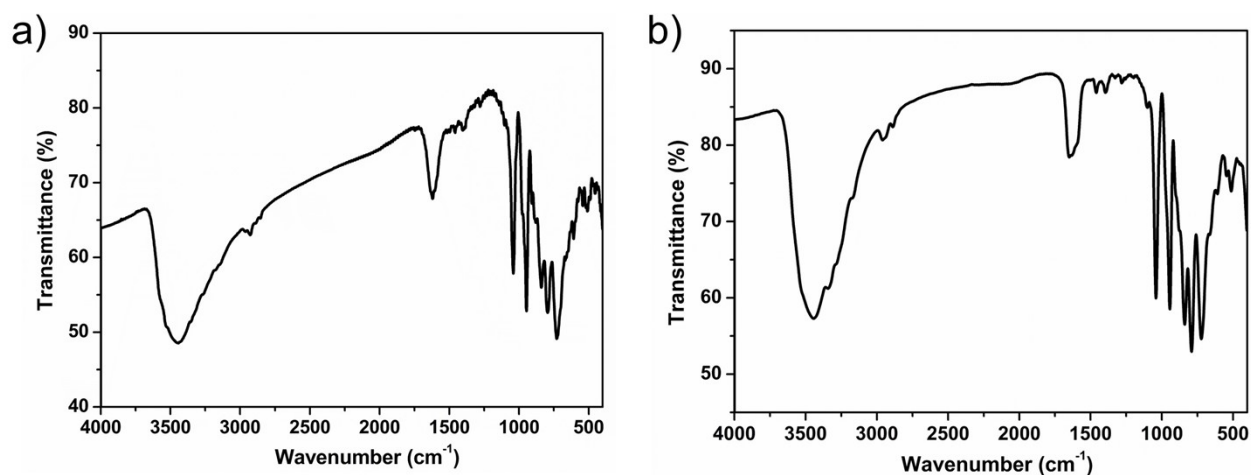
Fig. S11. The IR spectra of (a) **1** and (b) **2**.
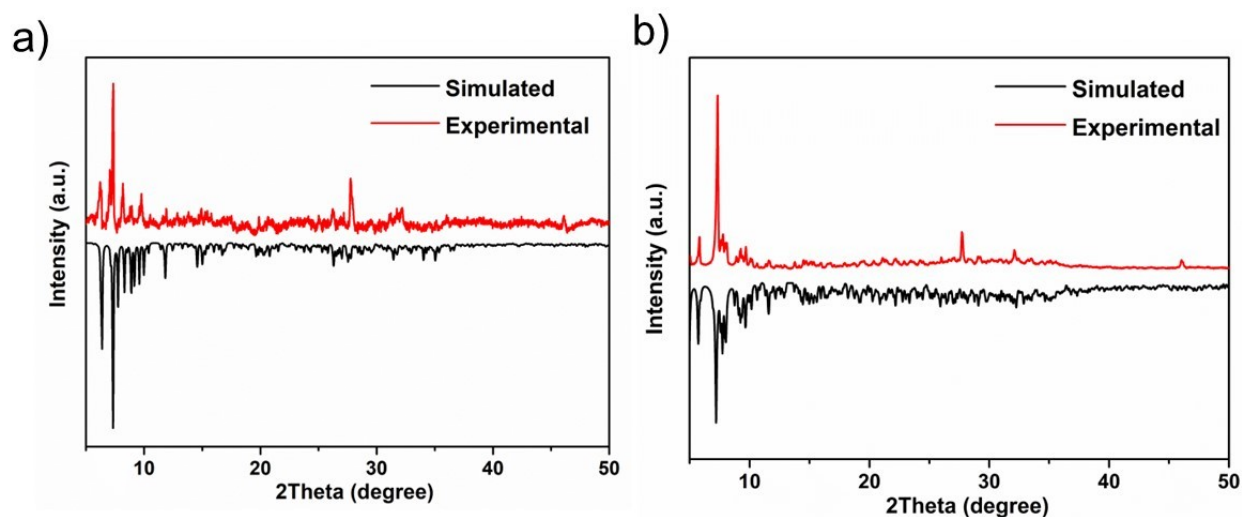
Fig. S12. Simulated and experimental PXRD patterns of (a) **1** and (b) **2**.

Thermogravimetric analyses. To evaluate the thermal stability of compounds **1** and **2**, the thermogravimetric analyses were tested from 25 to 700 °C (Fig. S13). The weight loss of both compounds can be regarded as a continuous process. From 25 to 640 °C, the reduction of 14.27% for the mass of compound **1** was attributed to the loss of 31 adsorbed water molecules, 39 lattice water molecules, 6 coordination water molecules, 10 enMe molecules and the dehydration of 8 protons (4 H_2O) and 8 OH^- groups (4 H_2O). The mass of compound **2** was reduced by 12.84% (calc. 12.95%) from 25 to 645 °C due to the loss of 45 lattice water molecules, 9 coordination water molecules, 10 en molecules, 4 enMe molecules and the dehydration of 9 protons (4.5 H_2O) and 8 OH^- groups (4 H_2O).
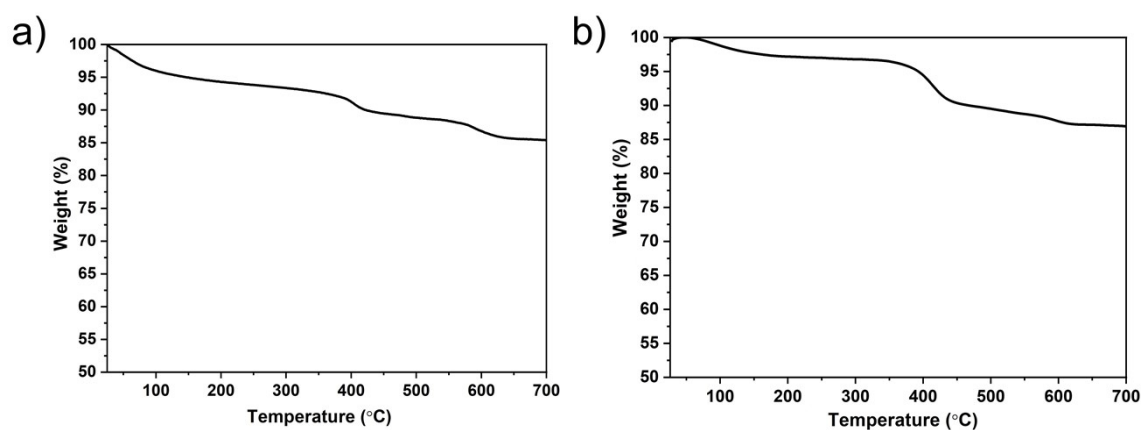

Fig. S13. The thermogravimetric analyses of compounds **1** and **2**.

Optical Band gaps. Fig. S14 shows the solid UV–vis diffuse-reflectance spectra of compounds **1** and **2** recorded from 200 to 800 nm. The ratio of α/S (α represents absorption coefficient, S represents scattering coefficient) was obtained according to the Kubelka–Munk formula: $\alpha/S = F(R) = (1-R)^2/(2R)$.[7] The band gap values of **1** and **2** were 3.41 and 3.32 eV, respectively, revealing the properties of semiconductors. The band gap values of **1** and **2** are similar to that of the reported NiAPs, such as $[Ni(enMe)_2(H_2O)_2][Ni_6(\mu_3\text{-}OH)_3(H_2O)_4(enMe)_3(CH_3COO)\text{-}(B\text{-}\alpha\text{-}PW_9O_{34})]_2\cdot10H_2O$ (E_g=3.75 eV) and $[Ni_6(\mu_3\text{-}OH)_3(H_2O)_2(dien)_3(B\text{-}\alpha\text{-}PW_9O_{34})]\cdot4H_2O$ (E_g=3.66 eV).[8]
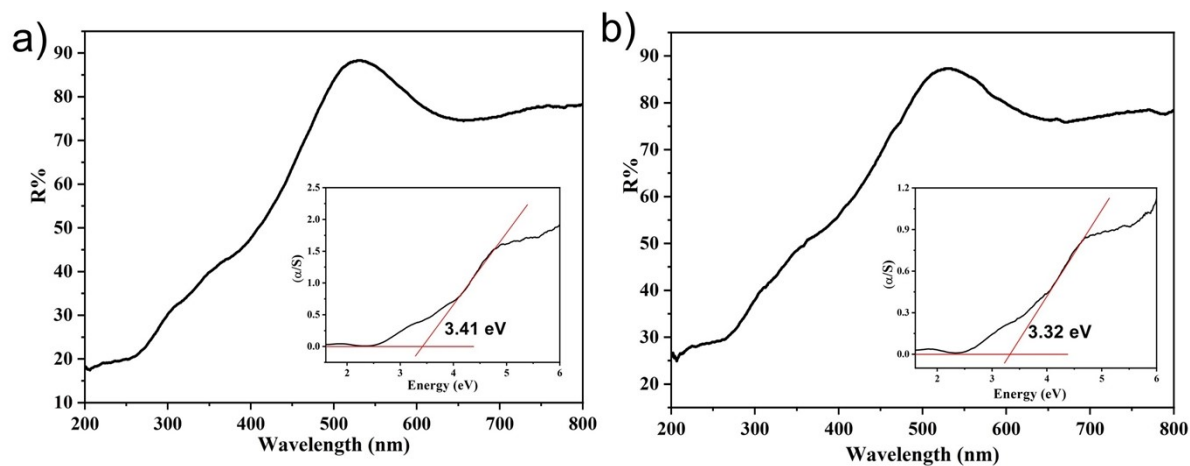
Fig. S14. The UV–Vis diffuse-reflectance spectra and (inset) the UV–Vis plots of Kubelka–Munk function versus energy E (eV) of compounds (a) **1** and (b) **2**.

Table S1. The BVS values of all Ni atoms and some selected O atoms in the compound **1**.

Atom1	Atom2	Bond length (Å)	Bond valence sum (BVS)	Atom1	Atom2	Bond length (Å)	Bond valence sum (BVS)
Ni1	O41	2.107		Ni8	N1	2.069	
Ni1	O41[1]	2.107		Ni8	N2	2.102	
Ni1	O43	2.027	1.99	Ni8	O48[1]	2.034	1.95
Ni1	O43[1]	2.027		Ni8	O58	2.110	
Ni1	O45	2.058		Ni8	O59	2.181	
Ni1	O45[1]	2.058		Ni8	O63	2.035	
Ni2	O25	2.061		Ni9	O28	1.991	
Ni2	O26	2.093		Ni9	O29	2.107	
Ni2	O27	2.053	1.84	Ni9	O31	2.098	2.00
Ni2	O30	2.265		Ni9	O37	2.065	
Ni2	O36	2.061		Ni9	O46	2.082	
Ni2	O40	2.057		Ni9	O3W	2.030	
Ni3	O52	2.088		Ni10	N5	2.070	
Ni3	O56	2.066		Ni10	N6	2.067	
Ni3	O57	2.020	2.01	Ni10	O25	2.083	1.99
Ni3	O58	2.017		Ni10	O33	2.152	
Ni3	O63	2.012		Ni10	O39	2.041	
Ni3	O65	2.172		Ni10	O40	2.070	
Ni4	N7	2.064		Ni11	N3	2.094	
Ni4	N8	2.073	1.99	Ni11	N4	2.079	1.90
Ni4	O27	2.088		Ni11	O55	2.042	
Ni4	O35	2.003		Ni11	O64	2.184	

Ni4	O36	2.139		Ni11	O66	2.077	
Ni4	O38	2.122		Ni11	O1W	2.114	
Ni5	O44[1]	2.109		Ni12	O29	2.057	
Ni5	O55	2.024		Ni12	O46	2.057	
Ni5	O59	2.073	1.88	Ni12	O56	2.045	2.01
Ni5	O63	2.021		Ni12	O57	2.033	
Ni5	O64	2.079		Ni12	O67	2.063	
Ni5	O65	2.224		Ni12	O2W	2.096	
Ni6	O55	2.026		Ni13	O27	2.043	
Ni6	O57	2.002		Ni13	O28	2.011	
Ni6	O65	2.172	2.02	Ni13	O30	2.146	2.03
Ni6	O66	2.037		Ni13	O34	2.050	
Ni6	O67	2.060		Ni13	O37	2.053	
Ni6	O79	2.069		Ni13	O38	2.041	
Ni7	O25	2.057		Ni14	N9	2.135	
Ni7	O28	2.005		Ni14	N9[2]	2.135	
Ni7	O30	2.168	2.01	Ni14	N10	2.094	1.89
Ni7	O31	2.055		Ni14	N10[2]	2.094	
Ni7	O32	2.062		Ni14	O54[2]	2.110	
Ni7	O33	2.028		Ni14	O54	2.110	
O25	Ni2	2.061		O55	Ni5	2.024	
O25	Ni7	2.057	2.01	O55	Ni6	2.026	1.08
O25	Ni10	2.083		O55	Ni11	2.042	
O25	Sb2	1.963		O57	Ni3	2.020	
O27	Ni2	2.053		O57	Ni6	2.002	1.12
O27	Ni4	2.088	2.02	O57	Ni12	2.033	
O27	Ni13	2.043		O63	Ni3	2.012	
O27	Sb1	1.965		O63	Ni5	2.021	1.11
O28	Ni7	2.005		O63	Ni8	2.035	
O28	Ni9	1.991	1.17				
O28	Ni13	2.011					

Table S2. Summary of some POM-based heterogeneous catalysts for H_2 evolution.

Catalyst formula	Photosensitizer	co-catalyst	Sacrificial electron donor	light	Activity ($\mu mol\ g^{-1}\ h^{-1}$)
$K_8Na_8H_4[P_8W_{60}Ta_{12}(H_2O)_4$-$(OH)_8O_{236}]\cdot 42H_2O$ [9]	None	Pt	CH_3OH	250W Hg lamp	1250
$Cs_{10.5}K_4H_{5.5}[Ta_4O_6(SiW_9Ta_3O_{40})_4]\cdot 30H_2O$ [9]					803
$K_6SiW_{11}O_{39}Ni(H_2O)\cdot 15H_2O$ [10]	None	Pt	zinc powders	500 W Xe lamp ($\lambda > 400$ nm)	98
$K_6SiW_{11}O_{39}Co(H_2O)\cdot 14H_2O$ [10]					65
$K_6SiW_{11}O_{39}Cu(H_2O)\cdot 14H_2O$ [10]					150

$K_6SiW_{11}O_{39}Zn(H_2O)\cdot15H_2O$ [10]					48
$[Cu^I_{12}(trz)_8(H_2O)_2]$-$[\alpha\text{-}SiW_{12}O_{40}]\cdot2H_2O$ [11]	None	Pt	CH_3OH	300 W Xe lamp	192.2
$Na_8Ta_6O_{19}/Cd_{0.7}Zn_{0.3}S$ [12]	None	None	Na_2S/Na_2SO_3	300 W Xe lamp	43050
$[Cu(en)_2]_6\{[Cu(en)_2]@\{[Cu_2(trz)_2\text{-}(en)_2]_6[H_{10}Nb_{68}O_{188}]\}\}$ [13]	$[Ir(ppy)_2(dtbbpy)][PF_6]$	None	TEOA	300 W Xe lamp ($\lambda>420$ nm)	381
$[Cu^{II}_5(2\text{-}ptz)_6(H_2O)_4(GeW_{12}O_{40})]\cdot4H_2O$ [14]	None	None	CH_3OH	Xe lamp	3813
$[Cu^I_2(ppz)_4][H_2GeW_{12}O_{40}]\cdot8H_2O$ [14]					500
$Cu_8(H_2O)_2(en)_4(B\text{-}\alpha\text{-}H_2\text{-}SiW_9O_{34})_2]$ [15]	$[Ir(ppy)_2(dtbbpy)][PF_6]$	None	TEOA	LED light (450 nm)	833.33
$[Ni(H_2O)_6]KH[NiMo_6O_{24}(Sb_3O_3)_2]\cdot5H_2O$ [16]	$[Ir(coumarin)_2\text{-}(dtbbpy)]^+$	None	TEOA	300 W Xe lamp (400 nm cutoff filter)	10358
$H_3[(btc)Ni_6(\mu_3\text{-}OH)_3(H_2O)_5(B\text{-}\alpha\text{-}PW_9O_{34})]\cdot17H_2O$ [17]	$[Ir(ppy)_2(dtbbpy)][PF_6]$	None	TEOA	white light (400−800 nm, 5 W)	1058.24
$H_6Na_8Cs_3[Co_9(\mu_3\text{-}OH)_3(H_2O)_6(HPO_4)_2(B\text{-}\alpha\text{-}PW_9O_{34})_3]Cl\cdot40H_2O$ [18]	$[Ir(ppy)_2(dtbbpy)][PF_6]$	None	TEOA	white light (400–800 nm, 10 W)	1217.6
Compound **2** (**this work**)	$[Ir(coumarin)_2\text{-}(dtbbpy)]^+$	None	TEOA	white light (400–800 nm, 10 W)	19214

References

[1] P. J. Domaille, G. Hervéa, and A. Téazéa, *Inorganic Syntheses*, 1990, **27**, 96.

[2] L. Qin, C. Y. Zhao, L. Y. Yao, H. B. Dou, M. Zhang, J. Xie, T. C. Weng, H. J. Lv and G. Y. Yang, *CCS Chem.,* 2022, **4**, 259.

[3] O. V. Dolomanov, L. J. Bourhis, R. J. Gildea, J. A. K. Howard and H. Puschmann, *J. Appl. Cryst.,* 2009, **42**, 339.

[4] G. M. Sheldrick, *Acta Cryst.,* 2015, **A71**, 3.

[5] G. M. Sheldrick, *Acta Cryst.,* 2015, **C71**, 3.

[6] B. Rees, L. Jenner and M. Yusupov, *Acta Cryst.,* 2005, **D61**, 1299.

[7] W. M. Wendlandt and H. G. Hecht, *Reflectance Spectroscopy*, Interscience: New York, 1966.

[8] S. T. Zheng, D. Q. Yuan, H. P. Jia, J. Zhang and G. Y. Yang, *Chem. Commun.,* 2007, **18**, 1858.

[9] S. J. Li, S. M. Liu, S. X. Liu, Y. W. Liu, Q. Tang, Z. Shi, S. X. Ouyang and J. H. Ye, *J. Am. Chem. Soc.,* 2012, **134**, 19716.

[10] Z. L. Wang, Y. Lu, Y. G. Li, S. M. Wang and E. B. Wang, *Chin. Sci. Bull.,* 2012, **57**, 2265.

[11] X. X. Zhao, S. W. Zhang, J. Q. Yan, L. D. Li, G. J. Wu, W. Shi, G. M. Yang, N. J. Guan and P. Cheng, *Inorg. Chem.,* 2018, **57**, 5030.

[12] X. J. Zhou, H. Yu, D. Zhao, X. C. Wang and S. T. Zheng, *Appl. Catal. B: Environ.,* 2019, **248**, 423.

[13] Z. K. Zhu, Y. Y. Lin, H. Yu, X. X. Li and S. T. Zheng, *Angew. Chem. Int. Ed.,* 2019, **58**, 16864.

[14] Q. B. Shen, C. J. Gómez-García, W. L. Sun, X. Y. Lai, H. J. Pang and H. Y. Ma, *Green Chem.,* 2021, **23**, 3104.

[15] J. J. Sun, W. D. Wang, X. Y. Li, B. F. Yang and G. Y. Yang, *Inorg. Chem.,* 2021, **60**, 10459.

[16] M. Z. Chi, H. J. Li, X. Xin, L. Qin, H. J. Lv and G. Y. Yang, *Inorg. Chem.,* 2022, **61**, 8467.

[17] Z. W. Wang, Q. Zhao, C. A. Chen, J. J. Sun, H. J. Lv and G. Y. Yang, *Inorg. Chem.,* 2022, **61**, 7477.

[18] Z. W. Wang and G. Y. Yang, *Molecules*, 2023, **28**, 664.